ACTA PHYSICA DEBRECINA XLVII, 163 (2013)

ANISOTROPIC MAGNETIC NANOPARTICLES - MORE EFFECTIVE HYPERTHERMIA FOR CANCER THERAPY?

J. Rácz[1,2], I. Nándori[2,3], J. Halász[4], P. F. de Châtel[3]

[1] University of Debrecen, H-4010 Debrecen P.O. Box 105, Hungary
[2] MTA Atomki, H-4001 Debrecen, P.O. Box 51. Hungary
[3] MTA-DE Particle Physics Research Group, H-4010 Debrecen P.O. Box 105, Hungary
[4] Vadaskert Hospital, H-1021 Budapest, Lipotmezei 1-5, Hungary

Abstract

The mechanism of magnetization reversal in single-domain ferromagnetic particles is of interest in many applications, in most of which losses must be minimized. In cancer therapy by hyperthermia the opposite requirement prevails: the specific loss power should be maximized. The research to be reported below is related to the investigation of the role of anisotropy in an anticipated enhancement of heat production of magnetic nanoparticles under circularly polarized external field.

I. Introduction

Hyperthermia has been widely studied as adjuvant therapy additional to standardized chemotherapy and radiotherapy in patients with different cancers. The term hyperthermia refers to temperature above 41 °C (somewhat between 41 and 45 °C), and the strategy seems promising in oncological terms as cancer cells partially lack proper recovery mechanisms (e.g. decreased amount of heat-shock proteins, HSP 70, HSP 27) during excessive heat conditions [1, 2]. During hyperthermic conditions, compared to physiological cells, cancer cells are more vulnerable to additional environmental

stressor, like cytotoxic agents and irradiation, and depending on the conditions, programmed cell death (apoptosis) or in certain cases necrosis might occur. A major technical problem is the selective heating of the tumor tissue without damaging its environment. Excessive heat conditions might have serious side effects (local or extended destruction of healthy tissues), thus proper control in the targeting, extension and duration of hyperthermia is inevitable for therapeutic applications [1].

Among many forms of hyperthermia, the local induction of hyperthermia via magnetic nanoparticles seems a fruitful strategy, with promising preclinical results in different cancer models [3]. The unique feature of magnetic nanoparticle hyperthermia is that the energy is transported in the body by means of an ac magnetic field. The nanoparticles absorb the energy, and the magnetic moment of the particles enable also targeting: they can be directed towards the cancer tumors by a magnetic field. Overheating might also be controlled by applying compounds with optimalized Curie temperature.

Local microinjection of magnetic nanoparticles for hyperthermia induction was repeatedly performed in patients with glioblastoma multiforme (a devastating brain tumor) [4] and in patients with prostate cancer [5], where the feasibility of other procedures were considerably low. In the above cases, little side-effects were present, and beneficial clinical effects were observed. Technically, the microinjection contained superparamagnetic iron oxid nanoparticles (measured approximately 15 nm in diameter) covered by aminosilane type shell. Systematic administration of iron oxid particles (like contrast agents in MRI settings) is regularly applied (so far not for therapeutical reason), and these molecules might also be used for local hyperthermia induction in case of increased local accumulation in the cancer tissue. At present the clinical application of the promising procedure is still limited, partly due to the efficacy of the heat transfer and controllability of temperature parameters [6]. Yet, the study of relaxation mechanisms of magnetic nanoparticles is a very active research field both in its theoretical and material-science aspects.

The research to be reported below follows our earlier investigation of the isotropic, single-particle case. This work [7] was based on the Landau-Lifshitz-Gilbert (LLG) equation and it was followed by a similar work based

on the modified Bloch equation [8]. Apart from finding the response of the magnetization of nanoparticles to an applied ac field, we have determined the frequency dependence of the energy loss (i.e. the heat gain). For both models, we found that, in the low-frequency limit, larger energy loss per cycle was achieved applying linearly, rather than circularly polarized field. However, as no magnetic particle is strictly isotropic, it is essential to study the anisotropic case. The purpose of our recent paper [9] was to determine the role of anisotropy in an anticipated enhancement of heat production of magnetic nanoparticles under circularly polarized field. Solving the differential equation, which describes the dynamics of the magnetization in circularly polarized field, we have found that the power losses decreased due to the anisotropy. The outcome of our research was then that in the low-frequency limit, in circulary polarized field, it is impossible to increase the energy loss using easy-axis, uniaxially nanoparticles.

The purpose of the present work is (i) to summarize the results on the anisotropic case [9] and (ii) to present new results calculated for higher frequencies than reported in [9], but still falling into the range allowed in hyperthermia.

II. The Landau-Lifshitz-Gilbert equation

Out of the many phenomenological equations of motion for the relaxation of magnetic moments or magnetization [10], the one put up by Landau and Lifshitz [11] and extended by Gilbert [12] into the realm of strongly damped moments has proved to give the most realistic description of the dynamics of single-domain magnetic particles. An important feature of the resulting Landau-Lifshitz-Gilbert (LLG) equation is that the magnetization vectors magnitude does not change under the influence of the external field. Thus, it is convenient to rewrite it in terms of the unit vector $\mathbf{M} = \mathbf{m}/m_S$ where m_S is the saturation magnetization. Then the LLG equation reads as

$$\frac{\mathrm{d}}{\mathrm{dt}}\mathbf{M} = -\gamma\,[\mathbf{M} \times \mathbf{H}_{\mathrm{eff}}] + \alpha\,[[\mathbf{M} \times \mathbf{H}_{\mathrm{eff}}] \times \mathbf{M}], \tag{1}$$

where γ and is related to the gyromagnetic ratio, but also depends on the damping, and α is a phenomenological damping constant, $\mathbf{H}_{\mathrm{eff}}$ contains the

circularly polarized applied (external) magnetic field and the effect of the anisotropy of the magnetic particle:

$$\mathbf{H}_{\text{eff}} = H_0 \ (\cos(\omega t), \sin(\omega t), \lambda_{\text{eff}} M_z), \tag{2}$$

where ω is the angular frequency of the applied field, M_z is the z-component of the normalized magnetization vector and λ_{eff} is the measure of the strength of the anisotropy with respect of the applied H_0 field. In this measure, using $\lambda_{\text{eff}} > 1$ (cf. Fig. 1, Fig. 2 and Fig. 4) and realizing that $\mathbf{M}$ is a dimensionless unit vector, we are aware of working with strong anisotropy.

Transforming the LLG equation into polar coordinates allows to drop the constant (M), leaving but two equations:

$$\frac{\mathrm{d}\theta}{\mathrm{dt}} = \omega_L \sin\phi + \alpha_N \cos\theta \cos\phi - \alpha_N \lambda_{\text{eff}} \sin\theta \cos\theta, \tag{3}$$

$$\frac{\mathrm{d}\phi}{\mathrm{dt}} = \omega_L \cos\phi \frac{\cos\theta}{\sin\theta} + w - \alpha_N \frac{\sin\phi}{\sin\theta} - \omega_L \lambda_{\text{eff}} \cos\theta. \tag{4}$$

Note that the new coordinate system is rotating with the applied field: the azimuthal angle (φ) has been cut into the rotation (ωt) and a measure (ϕ) of the lag of $\mathbf{M}$ with respect to the rotation of the applied field: $\varphi = \omega t - \phi$.

The left sides of equations (3) and (4) being derivatives of angles with respect to time, the units of all terms in the equations must be s^{-1} . Indeed, the first one on the right sides is the Larmor frequency, $\omega_L = |\gamma|\mu_0 H_0$ where $\gamma = 1.76 \times 10^{11}$ $\mathrm{Am}^2/\mathrm{Js}$ is the gyromagnetic ratio of the electron spin and $\mu_0 = 4\pi \times 10^{-7}$ $\mathrm{N/A}^2$ is the permeability of free space. Known that in the practice [14] $H_0 \leq 18$ kA/m we find that the Larmor frequency is of the order of GHz. In hyperthermia the frequency of the applied field is advised [15] to be chosen above about 100 kHz and below about 500 kHz, so that ω should be four orders of magnitude below ω_L. In the spirit of the Landau-Lifshitz approach, the damping constant $\alpha_N = |\gamma|\mu_0\alpha$ should be much smaller than ω_L. We shall show results of simulations made for $\alpha_N = \omega_L/2$, which can only be accepted if we assume that both γ and α are reduced by a factor of $(1+(\alpha/\beta)^2)^{-1}$ (where β is of dimension α) as it was done in [9], in accord with the procedure of moving from the Landau-Lifshitz equation to the Landau-Lifshitz-Gilbert equation. So far it seems that the Larmor precession dominates the equations of movements, but the

effect of anisotropy may very well have the same order of magnitude, or indeed larger: the anisotropy field of magnetite is more than 40 kA/m, and if we reckon with the shape anisotropy too, as suggested by Bertotti et al. [13], a much stronger effect can be expected.

III. Anisotropic case, low frequency

In this section we briefly summarize the results obtained for the anisotropic case in the low-frequency limit [9]. We have given numerical solutions of the equations of motion set up for uniaxial anisotropy (Eqs. (3), (4) and $\lambda_{\text{eff}} > 0$) in polar coordinates with various initial conditions in θ vs ϕ plots. To limit the number of Larmor circles before the steady state settles, the parameters we have chosen are unlike the ones encountered in hyperthermia: the Larmor frequency exceeds the applied frequency by factors of 4/3 to 20, instead of being four orders of magnitudes higher. As we are observing the motion in a frame rotating with the applied field, it is surprising that we see no sign of the Larmor precession before the orbits collaps in the attractive fixed point.

In Fig. 1, two fixed points, a repulsive (circle) one and an attractive one appear on the diagram. The lines carrying arrows, which indicate the passing of time, is what we call orbits, the figures being orbit maps. The attractive fixed point, where all orbits eventually arrive, indicate steady states. Garstens and Kaplan [16] have defined steady states in terms of the average value of M_z, i.e., $\cos(\theta)$, over one cycle, which must be time-independent. Clearly, with $\theta =$ constant, our fixed points represent steady states. In this case, with a counter-clockwise rotation of the applied field, the attractive fixed point is above the equator, the repulsive fixed points is very close to the equator. In ref. [9] we have reported the observation of parameter sets that supported two attractive fixed points; Fig. 2 is an example. Here we also marked the saddle point between the two fix points. In what follows, we shall seek the critical anisotropy strength, at which the second fixed point emerges. We define λ_{cr}, the critical value of the anisotropy strength λ_{eff}, as the one at which only one attractive fixed point appears, but the smallest increase, be it only a percent, will cause the appearance of a new attractive fixed point. Out of these attractive fixed points one is below the equator, the other one above.

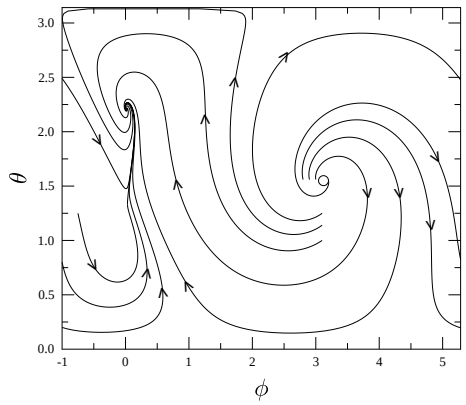

Figure 1: Orbit map in the rotating frame obtained by solving the LLG equation, slightly below the critical value of anisotropy. The parameters are $\alpha_N = 0.1$, $\omega = 0.01$, $\omega_L = 0.2$ and $\lambda_{\text{eff}} = 1.175$.

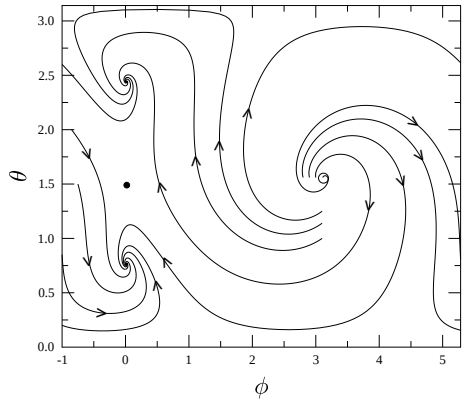

Figure 2: Orbit map in the rotating frame obtained by solving the LLG equation 28% above the critical value of anisotropy, $\lambda_{\text{eff}} = 1.5$. The other parameters are as under Fig. 1.

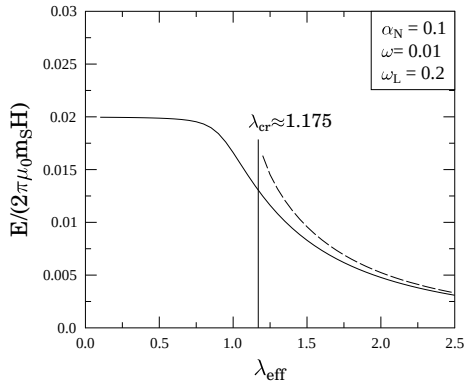

Figure 3: The energy loss is plotted against the anisotropy λ_{eff}. There are two scaling regimes, the one is at small, the other is at large anisotropy which are separated by critical value of anisotropy.

Fig. 3 shows the energy losses as functions of λ_{eff}. The solid line corresponds to the energy dissipated per particle in a single cycle at the stable fixed point, the dashed line refers to the fixed points which emerges at λ_{cr}. When calculating the energy loss, it is not clear which fractions of the contributions of the two fixed points have to be added. It is clear though that this is irrelevant in our search of means to enhance the energy loss. No matter which fixed point of the anisotropic particle, the isotropic particle's energy loss, represented by the straight line beginning at $\lambda_{\text{eff}} = 0$, is significantly higher. We must conclude that an easy-axis uniaxial anisotropic sample will never perform better in the dissipation of magnetic energy than its isotropical variant with otherwise the same magnetic parameters.

IV. Anisotropic case, medium frequency

Two intriguing features of the results shown in the previous section dictate the subject to be clarified before extend the construction and analysis of orbit maps. First, the existence and number of fixed points. Here the question of the possibility of more than two fixed points arises. Secondly, the asymmetry of Fig. 3 raises two questions: what prohibits the presence of the second fixed points in the case of weak anisotropy and what is the form and physical background of the dependence of the critical value of the

anisotropy strength $\lambda_{\rm cr}$ and the ratio of the applied and Larmor frequencies ω/ω_L?

Denisov and coworkers [17] have observed the asymmetry in the occurance and position of the two fixed point in the $\theta - \phi$ map. They pointed out that the rotating magnetic field breaks the symmetry between the directions pointing up and down the plane of rotation, i.e. the two equivalent directions of the uniaxial symmetry.

Lyutyy and coworkers [18] have stated that increasing the frequency should enhance the energy loss. To find out if this increase is significant within the frequency range allowed in hyperthermia, we have increased in three steps the applied frequency in numerical calculations of the orbit maps and the energy loss. The outcome supports the statement that raising the frequency improves energy loss. Furthermore, comparing the orbit maps of models differing only in the applied frequency leads to observations worthy to pursue in a broader context.

Fig. 4 shows the trends in the occurance and properties of the critical values of the anisotropy strength at different applied frequencies. Figure 1, where $\omega/\omega_L = 1/20$, is part of this series, where the ratio is raising up to $\omega/\omega_L = 3/4$. We see a growth of $\lambda_{\rm cr}$, monotonic (in fact almost linear) in ω/ω_L, from 1.175 to 2.2. This seems a large change, until we realize that between $\omega/\omega_L = 1/20$ and zero the change is 1.175. The behaviour of $\lambda_{\rm cr}$ in a wider and more varied area will be necessary to analyse these data.

Another feature of the second fixed points that we can observe in these figures is that both the values of the energy loss per cycle and the difference between these data for the two fixed points are increasing with increasing critical anisotropy. In Table 1 we have collected the data one can draw from the E vs $\lambda_{\rm eff}$ plots in Fig. 3 and Fig. 4.

Fig. 1 and especially the orbit maps in Fig. 4 draw the attention to another kind of special point or area: where a number of orbits seem to join in one, which then abruptly changes direction. Considering that $\lambda_{\rm eff}$ was chosen in these calculations very close to $\lambda_{\rm cr}$, the bends the orbits make before the union suggest that they were on their way to the second attractive fixed point. In a closer study of these points, including the velocities before and after them, may give a clue why the attraction disappears.

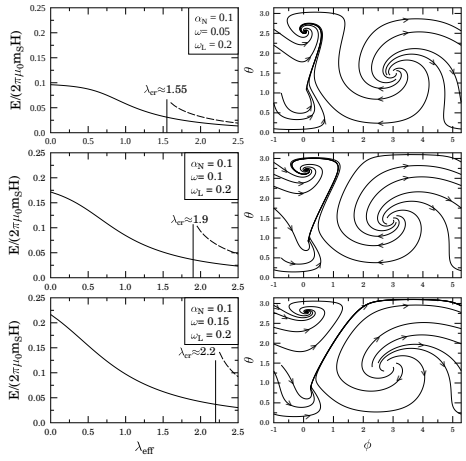

Figure 4: On the panels to the left, the energy loss is plotted against the anisotropy λ_{eff} for various values of ω (α_N and ω_L are fixed). On the panels to the right, one finds the corresponding orbit maps in the rotating frame obtained by solving the LLG equation, slightly below the critical value of anisotropy.

In conclusion, we have shown that orbit maps provide a tool to analyse the behaviour of single-domain magnetic particles. We have chosen to model easy-axis uniaxial ferromagnets in temperatures low enough to ignore thermal fluctuations. Expanding the parameter area and introducing time into the maps, we intend to use the method for models with parameters relevant to the usage of such nanoparticles in hyperthermia.

References

[1] B. Hildebrandt, P. Wulst, O. Ahlers, A. Dieing, G. Sreenivasa, T. Kerner, R. Felix and H. Riess, Crit. Rev. Oncol. **43** (2002) 33-56.

[2] G.C. Li and J.Y. Mak, Int. J. Hyperthermia **25** (2009) 249-257.

[3] B. Thiesen and A. Jordan, Int. J. Hyperthermia **24** (2008) 464-474.

ω	λ	E/cycle I.	E/cycle II.
0.01	1.175	0.013	0.0175
0.05	1.55	0.03	0.07
0.10	1.90	0.04	0.13
0.15	2.20	0.04	0.16

Table 1: Dependence of critical anisotropy and energy losses on the frequency of applied magnetic field at first and second fixed points. Data on four models with the same $\alpha_N = 0.1$ and $\omega_L = 0.2$ and ω given in first column.

[4] K. Maier-Hauff, F. Ulrich, D. Nestler, H. Niehoff, P. Wust, B. Thiesen, H. Orawa, V. Budach and A. Jordan, J. Neurooncol. **103** (2011) 317-324.

[5] M. Johannsen, B. Thiesen, P. Wust and A. Jordan, Int. J. Hyperthermia **26** (2010) 790-795.

[6] G. Bellizzi and O.M. Bucci, Int. J. Hyperthermia **26** (2010) 389-403.

[7] P. F. de Châtel, I. Nándori, J. Hakl, S. Mészáros and K. Vad, J. Phys.: Condens. Matter **21** (2009) 124202.

[8] Zs. Jánosfalvi, J. Hakl, P. F. de Châtel, arXiv:1201.5236 [cond-mat.mes-hall].

[9] I. Nándori, J. Rácz, Phys. Rev. E **86** (2012) 061402.

[10] R. Berger, J/C Bissey and J. Kliava, J. Phys.: Condens Matter **12** (2000) 9347.

[11] L. Landau and E. Lifshitz, Phys. Z. Sowjetunion **8** (1935) 153.

[12] T. L. Gilbert, Phys. Rev. **100** (1955) 1243.

[13] Giorgio Bertotti, Claudio Serpico, and Isaak D. Mayergoyz, Phys. Rev. Lett. **86** (2001) 724.

[14] M. Johannsen, U. Gneveckow, K.Taymoorian, C.H. Cho, B. Thiesen, R. Scholz, N. Waldöfner, S.A. Loening, P. Wust and A. Jordan, Actas Urol. Esp. **31** (2007) 660.

[15] S. E. Barry, Int. J. Hyperthermia **24** (2007) 451.

[16] M.A. Garstens and Kaplan, Phys. Rev. **99** (1955) 459.

[17] S. I. Denisov, T. V. Lyutyy, P. Hänggi, K. N. Trohidou, Phys. Rev. B **74** (2006) 104406.

[18] T. V. Lyutyy, S. I. Denisov, A. Yu. Polyakov, C. Binns, INTERNATIONAL CONFERENCE NANOMATERIALS: APPLICATIONS AND PROPERTIES **1** (2012) 04MFPN16.